

Published in final edited form as:

*Exp Cell Res.* 2005 July 1; 307(1): 194–203. doi:10.1016/j.yexcr.2005.03.026.

## Antisense inhibition of hyaluronan synthase-2 in human osteosarcoma cells inhibits hyaluronan retention and tumorigenicity

Yoshihiro Nishida<sup>1</sup>, Warren Knudson<sup>2</sup>, Cheryl B. Knudson<sup>2</sup>, and Naoki Ishiguro<sup>1</sup>

<sup>1</sup>Department of Orthopaedic Surgery, Nagoya University School of Medicine, 65 Tsurumai, Showa-ku, Nagoya 466-8550, Japan

<sup>2</sup>Department of Biochemistry, Rush Medical College, Rush University Medical Center, 1653 W. Congress Parkway, Chicago, IL 60612

### Abstract

Osteosarcoma is a common malignant bone tumor associated with childhood and adolescence. The results of numerous studies have suggested that hyaluronan plays an important role in regulating the aggressive behavior of various types of cancer cells. However, no studies have addressed hyaluronan with respect to osteosarcomas. In this investigation, the mRNA expression copy number of three mammalian hyaluronan synthases (HAS) was determined using competitive RT-PCR in the osteoblastic osteosarcoma cell line, MG-63. MG-63 are highly malignant osteosarcoma cells with an abundant hyaluronan-rich matrix. The results demonstrated that HAS-2 is the predominant HAS in MG-63. Accumulation of intracellular hyaluronan increased in association with the proliferative phase of these cells. The selective inhibition of HAS-2 mRNA in MG-63 cells by antisense phosphorothioate oligonucleotides resulted in reduced hyaluronan accumulation by these cells. As expected, the reduction in hyaluronan disrupted the assembly of cell-associated matrices. However, of most interest, coincident with the reduction in hyaluronan, there was a substantial decrease in cell proliferation, a decrease in cell motility and a decrease in cell invasiveness. These data suggest that hyaluronan synthesized by HAS-2 in MG-63 plays a crucial role in osteosarcoma cell proliferation, motility and invasion.

### Keywords

hyaluronan synthase; hyaluronan; MG-63; osteosarcoma

### Introduction

Osteosarcoma is the most common primary malignant tumor of bone [1]. It is a highly aggressive tumor composed of mesenchymal cells producing osteoid and immature bone that affects adolescents and young adults. The term osteosarcoma is used to describe a heterogeneous group of lesions with diverse morphology and clinical behavior. The current World Health Organization (WHO) classification of osteosarcoma recognizes three major subtypes of conventional osteosarcoma: osteoblastic, chondroblastic, and fibroblastic, reflecting the high level of microscopic variability of the tumor. The value of differentiating the above subtypes is unclear with mixed histologies frequently present in tumors.

---

Address all correspondence and reprint requests to: Yoshihiro Nishida, M.D., Department of Orthopaedic Surgery, Nagoya University School of Medicine, 65-Tsuruma, Showa, Nagoya, 466-8550, Japan, TEL: +81-52-741-2111(ext 5095), FAX: +81-52-744-2260, ynishida@med.nagoya-u.ac.jp.

Moreover, there is no convincing evidence of a difference in clinical behavior between the histologic subtypes. More understanding of the basic biology associated with heterogeneous cancers such as osteosarcoma may provide novel tools for treatment. The prognosis for osteosarcoma has been improved with the introduction of chemotherapy. However, current response rates cannot be improved with dose escalation as drug resistance limits further effectiveness. Therefore, there is a clear and critical need to develop new and alternative strategies for patients with osteosarcoma.

Hyaluronan (HA) is a high molecular weight linear glycosaminoglycan comprised of repeating disaccharide units, glucuronic acid and *N*-acetylglucosamine. HA is an abundant component of the extracellular matrix. Moreover, changes in the deposition of HA have been shown to regulate matrix assembly, cell migration, differentiation and proliferation [2]. For example, HA deposition increases during active tissue remodeling, e.g., during morphogenesis and wound healing [2]. Furthermore, HA binding proteins control these cellular behaviors through interactions with HA and assembly of pericellular matrices [2]. Increased HA levels are also observed in malignant tumors, which include gastric cancer, colorectal cancer, breast cancer, glioma, lung carcinoma and ovarian cancer [3–9]. Studies in vitro have demonstrated that HA levels correlate with the invasive and metastatic capacity of tumor cells [10]. Increased matrix deposition of HA may promote invasion by providing a suitable environment for cancer cells [3], stimulating cell motility via interactions with cell surface receptors of HA [11] as well as forming a barrier for cancer cells against host immunocompetent cells [12].

Three mammalian HAS genes have been cloned, designated *HAS-1*, *HAS-2* and *HAS-3* [13]. These three genes display sequence homology and share common exon-intron boundaries between exons 2 and 3 [14], yet, they are localized on separate chromosomes [15]. The existence of three homologous HAS genes suggests the possibility of genetic manipulation of cellular HA production. Several recent studies have shown that transfection of cells with expression plasmid vectors for HAS alters the behavior of tumor cells. Transfection of human fibrosarcoma cells with *HAS-2* stimulated both anchorage-independent growth and tumorigenicity [16]. In mouse mammary cancer cells, which had low levels of HA synthesis and displayed low metastatic capacity, high metastatic activity could be restored following transfection of the cells with an expression vector for *HAS-1* [17]. The introduction of the *HAS-1* and *HAS-2* genes promoted the growth of subcutaneous tumors dependent on the levels of hyaluronan synthesis [18]. Transfection of prostate cancer cells with a *HAS-3* expression vector resulted in elevated extracellular HA deposition, enhanced tumor cell growth and angiogenesis [19]. These studies suggest that hyaluronan synthesized by *HAS-1*, *HAS-2* or *HAS-3* play crucial roles in tumorigenicity. However, which HAS gene is predominantly responsible for the synthesis of hyaluronan in a specific tumor type is not well known and when it is known, there is little consensus for the utilization of *HAS-1*, *HAS-2* or *HAS-3*. Much of this work has been hampered because it has not been possible to generate specific monoclonal or polyclonal antibodies. Our previous work, using competitive-quantitative RT-PCR, characterized the mRNA copy numbers of HAS genes expressed by articular chondrocytes and demonstrated that *HAS-2* was the predominant enzyme responsible for the synthesis of HA in articular cartilage [20]. This same technique of accurately determining mRNA copy numbers of HAS genes allows us to characterize which HAS gene is primarily responsible for the synthesis of HA in various kind of tumors.

In this study, we determined the mRNA copy numbers of HAS genes expressed by the osteoblastic osteosarcoma cell line, MG-63. The results indicate that *HAS-2* was the predominant mRNA species expressed by the MG-63 cells. To confirm this result, and more importantly, to determine the potential roles played by HA in osteosarcoma cell tumorigenicity, specific antisense *HAS-2* phosphorothioate oligonucleotides were applied to

the MG-63 cells. HAS-2 antisense-treated cells were analyzed for changes in HAS mRNA gene expression, synthesis and retention of HA, cell proliferation, cell motility and cell invasiveness.

## Materials and Methods

### Reagents

Dulbecco's modified Eagles medium, trypsin EDTA, Trizol reagent for RNA isolation and lipofectamine reagent for transfection were obtained from Gibco BRL (Grand Island, NY). Fetal bovine serum (FBS) was purchased from Summit Biotechnology (Ft. Collins, CO). Gene Amp RNA PCR kit for reverse transcription-polymerase chain reaction was purchased from Perkin-Elmer (Norwalk, CT). Specific primers for HAS-1, HAS-2, HAS-3, and GAPDH were custom made by Integrated DNA Technologies (Coralville, IA). SYBR Green I gel stain was purchased from Molecular Probes (Eugene, OR). The phosphorothioate DNA oligonucleotides were synthesized by Oligos, Etc. (Wilsonville, OR) or Krabo (Osaka, Japan). Biotinylated hyaluronic acid binding protein was purchased from Seikagaku America (Falmouth, MA). Streptavidin peroxidase (component of Vectastain ABC kit) was purchased from Vector Laboratories (Burlingame, CA). Agarose was from FMC BioProducts (Rockland, ME). Cell Proliferation Kit I was purchased from Roche (Mannheim, Germany). Transwell<sup>®</sup> with 12.0 $\mu$ m pore size was purchased from Corning Inc. (Corning, NY). Matrigel was purchased from BD Biosciences (Bedford, MA). All other enzymes and chemicals either molecular biology grade or reagent grade materials were purchased from Sigma Chemical Co. (St. Louis, MO).

### Cell Culture

MG-63 cells (human osteoblastic osteosarcoma cell line) from American Type Culture Collection (ATCC) were maintained at 37°C in an atmosphere with 5% CO<sub>2</sub> with DMEM, supplemented with 10% FBS, penicillin and streptomycin. The cells were detached from the culture plate by treatment with 0.25% trypsin/EDTA. The cells were washed in DMEM containing 10% FBS to inactivate trypsin activity followed by a wash with serum-free DMEM. Cells were then resuspended in serum-free DMEM containing the presence or absence of various phosphorothioate oligonucleotides and replated into 35 mm dishes as monolayer cultures at a concentration of  $5 \times 10^5$  cells/dish for HA staining and particle exclusion assay, into 96-well plate at a concentration of  $5 \times 10^3$  cells/well for cell proliferation assay, and into Transwells<sup>®</sup> with 12.0  $\mu$ m pore size at a concentration of  $5 \times 10^5$  cells/well for cell invasion assay or motility assay. To provide for optimal transfection, the phosphorothioate oligonucleotides were first mixed with 6.0  $\mu$ g/ml lipofectamine in serum-free DMEM and incubated 20 minutes at room temperature to allow DNA-liposome complexes to form. The diluted complex solution (final oligonucleotide concentration of 2  $\mu$ M) was mixed gently and added to the cells at the time of plating. Medium containing antisense or control, sense oligonucleotides was then removed from the cultures after 5 hours of incubation and replaced with fresh DMEM containing 10% FBS (i.e., oligonucleotide-free medium) and incubation continued for varying periods of time.

### Phosphorothioate Oligonucleotides

HAS-2 antisense oligonucleotides were designed as 16-oligonucleotide sequences complementary to regions including the AUG start site of published human HAS-2 sequence: 5'-GCA TCT TGT TCA GCTC-3' [20]. Control oligonucleotides included a sense and a reverse sequence oligonucleotide complementary to the same region (sense: 5'-GAG CTG AAC AAG ATGC-3', reverse: 5'-CGT AGA ACA AGT CGAG-3'), as well as a scrambled sequence oligonucleotide (5'-CTT ACC TCA GTT ACAA-3').

## Staining for HA

Cultured MG-63 cells were fixed with 2% paraformaldehyde buffered with phosphate buffer saline (PBS) at room temperature for 2 hours. The cells were treated with 0.3% H<sub>2</sub>O<sub>2</sub> in 30% methanol for 30 minutes at room temperature to block the internal peroxidase activity, then incubated with 1% bovine serum albumin (BSA) in PBS for 1 hour at room temperature. Cells were then incubated with 2.0 µg/ml of a biotinylated HA binding protein (HABP) probe for 2 hours at room temperature. HABP binds to HA with high affinity and specificity (similar to an antibody) with a minimum binding site of ~41 HA monosaccharides [21]. Bound HABP was detected by the addition of streptavidin-peroxidase reagents (*Vectastain* kit) and diaminobenzidine-containing substrate solution (*SIGMA FAST™ DAB*). As a control, cells were pretreated with 5 units/ml *Streptomyces* hyaluronidase for 1 hour at 60 °C. Cultured cells were also stained with 4', 6-diamidino-2-phenylindole dihydrochloride hydrate (DAPI) and the nuclei visualized by fluorescent microscopy.

## Particle Exclusion Assay

Cell-associated pericellular matrices were visualized using a particle exclusion assay [22]. Briefly, following the 5 hour treatment of monolayer cultures of MG-63 cells with various phosphorothioate oligonucleotides and 11 or 35 hours of recovery in oligonucleotide-free medium, the culture medium was removed and replaced with a 0.75-ml suspension of formalin-fixed erythrocytes (10<sup>8</sup> per ml) in PBS containing 0.1% BSA. The particles were allowed to settle for 15 minutes. The cells were observed and photographed with an inverted phase-contrast microscope with *Varel* optics (*Zeiss*, Thornwood, NY). Morphometric analysis of randomly selected cells captured as digital images were analyzed using *Spot-RT* imaging software (*Diagnostic Instruments*). A matrix:cell ratio was defined as the ratio of the area delineated by the cell-associated matrix to the area delineated by the plasma membrane. If no detectable matrix is present the matrix:cell ratio would be 1.0.

## Reverse Transcriptase Polymerase Chain Reaction (RT-PCR): Conventional RT-PCR and Quantitative Competitive RT-PCR

Total cytoplasmic RNA of cultured MG-63 cells was extracted with *Trizol* reagents and subjected to reverse transcription and quantitative competitive PCR. Briefly, 0.125 µg of total RNA was converted to cDNA using Molony murine leukemia virus reverse transcriptase in the presence of 0.15 µM HAS-2 or HAS-3 specific downstream primers (HAS-2: 5'-TTT CTT TAT GTG ACT CAT CTG TCT CAC CCG-3', HAS-3: 5'-CAG AAG GCT GGA CAT ATA GAG GAG GG-3'). DNA fragments that share the same primer template sequence with the target cDNA but, contain a completely different, larger intervening sequence, were prepared and used as DNA internal standards (i.e., mimics) [20]. Aliquots of sample cDNA mixed together with serial dilutions of DNA mimics were co-amplified as templates in the presence of downstream primers and 0.15 µM upstream primers for HAS-2 or HAS-3 (HAS-2: 5'-ATT GTT GGC TAC CAG TTT ATC CAA ACG G-3', HAS-3: 5'-AGA GAC CCC CAC TAA GTA CCT CCG-3'), in a PCR mixture consisting of 2 mM magnesium chloride, 200 µM of each deoxyribonucleotide, and 2.5 units of *AmpliTaq* DNA polymerase. The DNA was denatured by heating at 95°C for 2 minutes, followed by 26 cycles of 1 min at 95°C, annealing at 60°C, and extension at 72°C for 1 minute (*Perkin Elmer* thermocycler). This reaction was followed by a final elongation step that lasted 5 minutes at 72°C. The amplified products were analyzed by electrophoresis on 1.5% agarose gels followed by staining with SYBR Green I. The stained products were scanned and quantified using a fluoroimaging system (*Molecular Dynamics*).

To determine that all samples contained equivalent amounts of RNA (i.e., to normalize results), in a separate set of reactions total RNA from samples were co-amplified in the

presence of serial dilutions of an RNA internal standard (mimic) prepared for glyceraldehyde-3-phosphate dehydrogenase (GAPDH). The GAPDH RNA mimic shares the same primer template sequence but contains a smaller intervening sequence. Samples containing 0.125 µg of sample total RNA were co-reverse transcribed with 2-fold serial dilutions of GAPDH RNA mimic in the presence of 0.15 µM GAPDH-specific downstream primer (5'-TTA CTC CTT GGA GGC CAT GTG GGC C-3'). The sample and mimic cDNA products were then co-amplified in the presence of the GAPDH-specific downstream primer together with 0.15 µM upstream primer (5'-ACT GCC ACC CAG AAG ACT GTG GAT GG-3') using PCR conditions as described for HAS-2 amplification. For conventional RT-PCR, HAS-1 specific primers (upstream: 5'-GGA CTA CGT GCA GGT CTG TGA CTC-3', downstream: 5'-ACT TGG TAG CAT AAC CCA TGC TGA G-3') were used as described for HAS-2, HAS-3, and GAPDH primer pairs and amplified for 35 cycles. As a positive control for HAS-1 mRNA expression, total RNA isolated from human synovial cells were used.

### Proliferation Assay

Cell proliferation was measured by the 3-(4,5-dimethylthiazol-2-yl)-2,5-diphenyl tetrazolium bromide (MTT) colorimetric assay 24 or 48 hours after treatment. Preliminary studies demonstrated that at 48 hours the cultures remained subconfluent and generated values within the linear, optimal ranges of the MTT assay. Microscopic inspection of the wells confirmed that decreased absorbance values correlated with decreased cell number. Color intensity was determined on a microculture plate reader at 570 nm. The data presented are the means ± s.d. from triplicate wells per microtitre plate with three replicate microtitre plates per experiment.

### Matrigel Invasion and Motility Assays

Chemotactic motility of MG-63 cells was investigated using 24-well cell culture chambers containing inserts with 12 µm pores. Invasion of osteosarcoma cells was assayed in the same chambers that also contained a reconstituted extracellular matrix (ECM) supported on the membrane (Matrigel layered on a 12 µm pore membrane). Five hours post-transfection with phosphorothioate oligonucleotides, the MG-63 cells were washed and then added to the upper chamber ( $5 \times 10^5$  cells/300 µl DMEM/well) and 900 µl of chemotaxis buffer including 10 µg/ml of fibronectin was placed in the lower chamber. After incubation for 12 or 24 hours at 37°C and 5% CO<sub>2</sub>, cells on the upper surface were wiped off with a cotton swab. Migrating and invading cells on the lower surface of the membrane were stained with hematoxylin. Cells from 4 different fields were counted under the light microscope using a magnification of 200x.

### Statistical analysis

Data of the cell proliferation, motility and invasion assay were analyzed by means of a Student *t*-test. A *P* value of less than 0.05 was considered to be significant.

## Results

### HAS mRNA expression in MG-63 cells

Only HAS-2 and HAS-3 products were detected following 35 cycles of conventional RT-PCR using MG-63 RNA (Figure 1A, lanes 2 and 3). HAS-1 mRNA expression was not detected in this cell line (Figure 1A, lane 1), whereas the same primer pairs successfully generated HAS-1 product from RNA derived from human osteoarthritic synovial cells (data not shown). To determine the copy numbers of HAS-2 and HAS-3 mRNA, quantitative, competitive RT-PCR was performed. Figure 1B is the co-amplification of target cDNA with

2-fold dilutions of mimic for HAS-2 (lanes 1–4) and HAS-3 (lanes 5–8). The deduced copy number for HAS-2 expressed in MG-63 ( $13.5 \pm 3.8 \times 10^8$  copies per  $\mu\text{g}$  total RNA) was approximately 90-fold higher than that of HAS-3 ( $0.146 \pm .05 \times 10^8$  copies per  $\mu\text{g}$  total RNA). Thus, by analysis of mRNA copy number, the data suggests that HAS-2 is the predominant enzyme responsible for the synthesis of HA in MG-63.

### HAS mRNA levels following the treatment of antisense oligonucleotides

As an approach to validate HAS-2 as the predominant HAS enzyme, the MG-63 cells were transfected with HAS-2 antisense phosphorothioate oligonucleotides. Inhibition of HAS-2 mRNA expression in MG-63 cell culture was confirmed by quantitative competitive RT-PCR (Figure 2). However, in these experiments, given that comparisons were being made between MG-63 cultures treated under varying conditions, the results of HAS mRNA copy number was normalized by GAPDH copy numbers (data not shown). As shown in Figure 2 and summarized in quantitative form in Table 1, treatment of MG-63 cells with antisense oligonucleotides resulted in an 54% inhibition of HAS-2 mRNA copy number expression 16 hours after treatment, as compared with cells treated with the control sense oligonucleotides. Similar control values were obtained for cultures treated with reverse or scrambled oligonucleotides (data not shown). At the 40 hour time point, HAS-2 mRNA levels in antisense-treated cultures were still inhibited by 43% as compared with the cultures treated with sense oligonucleotides. To confirm the specificity of HAS-2 antisense oligonucleotide induced inhibition, HAS-3 mRNA levels were also evaluated by quantitative competitive RT-PCR. As shown in Figure 2 and Table 1, MG-63 cultures treated with antisense and sense oligonucleotides at both time points exhibited less than a 10% difference in HAS-3 mRNA levels. A decrease in HAS-3 copy number at the 40 hour time point compared with values observed at 16 hours was noted however, this decrease was observed in both sense and antisense-treated cultures.

### Relationship between proliferation phase of MG-63 and HA accumulation

The relationship between HA accumulation in the cytoplasm, on the cell surface, and in pericellular matrix of MG-63 cells during various phases of proliferation is unknown. Biotinylated HABP was used to visualize HA accumulation of MG-63 cells during the exponential growth phase and in confluent cultures. As shown in Figure 3A, MG-63 cells in the exponential growth phase display prominent staining for HA within both the cytoplasm (arrows) and the cell-associated matrix. The intracellular staining provides a contrast outline of the cell nucleus (compare Figure 3A and 3B). However, at confluence (Figure 3C) the cells in confluent culture exhibit decreased HA-positive staining as compared with the cells in the exponential growth phase. Additionally, as less HA is now found intracellularly the visualization of the nuclei (seen in Figure 3D) is no longer apparent.

### Antisense inhibition of HAS-2 inhibits HA accumulation

Biotinylated HABP was also used for visualize HA accumulation after treatment of MG-63 cells with HAS-2 antisense oligonucleotides. As shown in Figure 4B and 4D, cells treated with control sense oligonucleotides for 12 and 24 hours respectively, display prominent staining for HA within both the cell cytoplasm and cell-associated matrix. Given that the entire cell-associated matrix was removed by trypsin/EDTA treatment at the time of plating, the observed accumulation of HA in cell-associated matrix must represent newly synthesized HA. Cells treated with antisense HAS-2 oligonucleotides for the same time periods displayed a substantial inhibition of cell-associated HA and faint staining in the cell cytoplasm (Figure 4A; 12 hours and 4C; 24 hours). The expression of HA was not completely abrogated after treatment of antisense oligonucleotides, with the cells still exhibiting about half the staining intensity of control cells. However, these results are consistent with the 54% inhibition of HAS-2 mRNA (Table 1).

### Antisense inhibition of HAS-2 inhibits cell-associated matrix assembly

One of the functions of HA in tumor cells, as well as other connective tissue cells such as chondrocytes, is to serve as a scaffold for the assembly of a cell-associated matrix [2, 21]. Depletion of HA results in the suppression of cell-associated matrices in articular chondrocytes [20]. These matrices may favor independent cell growth. Many of the control tumor cells (16 hours post transfection with sense oligonucleotides) display prominent cell-associated matrices (Figure 4F) albeit with significant cell-cell variability (matrix:cell ratio of  $2.5 \pm 1.5$ ). However, HAS-2 antisense oligonucleotides treatment for 16 hours resulted in a uniform, near total inhibition of cell-associated matrix assembly (Figure 4E, matrix:cell ratio of  $1.1 \pm 0.1$ ). Forty hours post transfection, the cell-associated matrix diameter of the cells treated with antisense HAS-2 oligonucleotides began to increase in some cells; however, the population as a whole continued to fail to assemble prominent matrices (Figure 4G, matrix:cell ratio of  $1.6 \pm 0.9$ ). In contrast, the control cultures (sense-oligonucleotide-treated) at the same time point uniformly exhibited large cell-associated matrices, typical of MG-63 cells (Figure 4H, matrix:cell ratio of  $2.9 \pm 0.6$ ). By 72 hours there was no difference between control sense and antisense treated cells (data not shown).

### Effect of antisense HAS-2 oligonucleotides on cell proliferation

Figure 3 suggests that the MG-63 cells accumulate more HA during the proliferative phase of growth. If this accumulation of HA is causal in nature, inhibition of HA synthesis may inhibit cell proliferation. As shown in Figure 5, HA inhibition following treatment of MG-63 cells with HAS-2 antisense oligonucleotides (open bars) resulted in the statistically significant decreased proliferation as compared with the cells treated with sense oligonucleotides (shaded bars). A small but significant 13% inhibition of cell proliferation was observed 24 hours post transfection ( $p=0.012$ ). However, by 48 hours post transfection, when maximal inhibition of HA is observed, there was a 38% inhibition ( $p=0.0002$ ). Inhibition of cell proliferation was consistent with the level of HAS-2 antisense inhibition shown in Table 1. Control cultured cells without treatment of oligonucleotides display similar proliferation as sense oligonucleotides-treated cells (data not shown).

### Effect of HAS-2 antisense oligonucleotides on cell migration and invasiveness

Changes in the cell motility of MG-63 cells were evaluated by conventional Boyden chamber assays. Change in cell invasiveness was evaluated using a modified Boyden chamber assay that included a required invasion through Matrigel. The average number of cells ( $\pm$  s.d., taken from 4 fields of view), observed on the lower membrane are summarized in Figure 6, panels A and B. A substantial, 73% and 82% reduction in cell migration was observed in antisense treated cells (Figure 6A, open bars) at both 12 and 24 hour time points, respectively, as compared with control sense-treated cells (shaded bars;  $p=0.0066$  and  $p=0.00065$ , respectively). In the invasion assay, cells treated with antisense or control oligonucleotides did not exhibit successful invasion through the Matrigel at the 12 hour time point (Figure 6B). However, by 24 hours antisense treatment of MG-63 cells (Figure 6B, open bars) affected an 84% inhibition of cell capacity to pass through Matrigel-coated filters as compared to control, sense-treated cells (shaded bars;  $p=0.013$ ).

## Discussion

HA is associated with a wide variety of malignant tumors and has been implicated in cancer progression [3–9]. However, the importance of HA in osteosarcoma has not yet been investigated in terms of basic or clinical relevance. HA forms a base scaffold for the tethering of proteoglycans and other macromolecules important to the assembly of extracellular and pericellular matrices [3]. Such matrices are a common feature of osteosarcoma cells. To explore whether the expression of HA and pericellular matrices are

important to the aggressive behavior of osteosarcoma cells, the osteoblastic osteosarcoma cell line MG-63, (cells with an abundant cell-associated matrix) were used for the analysis of HA-dependent cell activities.

Previous reports investigating HAS expression in malignant cells were based on semi-quantitative method such as RT-PCR [23], without the determination of the mRNA copy number of each HAS isoform. In this study, absolute copy number of HAS mRNA expression was determined in the proliferative phase of MG-63 based on quantitative, competitive RT-PCR, and HAS-2 was found to be the predominant HA synthase mRNA in MG-63. The mRNA expression levels of HAS-3 did not change after treatment of cells with HAS-2 antisense oligonucleotides, suggesting that HAS-3 does not compensate (at the transcriptional level) for the inhibition of HAS-2. There was no expression of HAS-1 mRNA in MG-63 cells under all treatment conditions. Given that HAS-2 antisense oligonucleotides affected a proportional reduction in the deposition of HA, it is likely that HAS-2 is the predominant HA synthase present in these osteosarcoma cells. However, it will be necessary to analyze the effects of treatment of antisense oligonucleotides for HAS-3 on MG-63 cells to completely rule out the contribution of this other HA synthase but, considering that the absolute copy number of HAS-3 mRNA is ~100-fold lower than HAS-2 mRNA, the contribution of HAS-3 to the synthesis of HA in these cells is likely to be minimal.

MG-63 cells in the proliferative phase express abundant cytoplasmic HA compared with the cells in confluent culture, supporting the previous observation that intracellular HA levels increase during cell division [24]. In the current study, inhibition of HAS-2 mRNA expression resulted in the reduction of HA positive staining in the cytoplasm of MG-63 cells as well as a reduction of the cell-associated matrix. Mechanisms for the reduction of cytoplasmic HA in this study remain unclear. One possibility may be that amount of receptor-mediated internalized HA, via such receptors as CD44 [25] is also reduced due to the reduction of HA synthesis. It has also been suggested that HA in cells may be derived from an intracellular source [26].

Decreased HA deposition in both the cytoplasm and cell-associated matrix was coincident with the reduced proliferation in antisense treated cells. Recent studies have shown that extracellular HA strongly promotes cancer cell growth via interaction with CD44 [27], since HA activates the PI3K-AKT signaling pathway [28], which promotes cell survival. Disruption of these interactions between HA and tumor cells using small HA oligomers induces the attenuation of signaling [29], indicating the important roles of extracellular HA in cell proliferation. On the other hand, recent studies have shown that intracellular HA binding proteins as well as intracellular HA may have important roles in regulation of cell cycle or in gene expression [30]. More studies are necessary to elucidate the roles of HA, especially of intracellular HA, in cell growth and motility.

In this study, synthesis of endogenous HA was inhibited, resulting in the depletion of both cytoplasmic and cell-associated HA, and inhibition of cell proliferation and motility. It has also been suggested that both extracellular and intracellular HA have crucial roles in cell motility via interaction with cell surface receptors such as CD44, RHAMM and ICAM-1, and rapid uptake of exogenously added HA[31].

Many researchers have also demonstrated the important roles of HA for invasion. Assembly of HA-rich, hydrated matrices around the cells stimulates migration [32] and tumor cell-HA interactions mediated through CD44 may play roles in facilitating migration through the tumor associated HA-rich matrix[3]. Formation of hydrated, HA-rich matrix was disrupted in antisense treated cells, as visualized by the particle exclusion assay, resulting in reduced

motility and invasiveness in this study. These results are in accordance with the previous observations. Thus, inhibition of HA deposition by antisense treatment may inhibit cell motility via the disruption of the functional cell-associated matrix in MG-63 cells.

Other mechanisms of inhibitory effects by HAS-2 antisense treatment on cell invasiveness might involve reduced activity of matrix metalloproteinases, such as MMP-2 and MMP-9. The interaction between HA and CD44 on the cell surface of glioma stimulates the production of MMP-9 [33]. Other studies demonstrated the interaction between HA, its receptors and cytoskeleton, causing cytoskeletal change that promote migration and invasion. HA-mediated tumor cell migration is promoted via interaction between cytoplasmic tail of CD44 and ankyrin in ovarian tumor [34]. The details of the above steps have not been well elucidated, and further analysis is also necessary in this area.

Prognosis of osteosarcoma has been dramatically improved with the introduction of multi-agent chemotherapy. However, a number of patients still develop distant metastasis resulting in poor prognosis. Research has been focused on identifying reliable prognostic factors. Axial lesions have an inferior outcome [35, 36] and the presence of clinically detectable primary metastatic disease correlates with poor prognosis [35, 37]. Protein expression in serum, such as levels of LDH or alkaline phosphatase correlate with outcome [1, 38] and other molecular markers are also being investigated to determine the relative significance for predicting prognosis [39, 40]. Considering that the major purpose of cancer biology research is to identify prognostic factors and therapeutic targets, obtaining a better knowledge of molecular pathology in osteosarcoma is continuously needed.

Conventional osteosarcoma can be divided into groups (e.g., osteoblastic, chondroblastic, fibroblastic), reflecting the predominant type of matrix in the tumor[41]. Thus, matrix in osteosarcoma is heterogeneous among tumors, leading us to the hypothesis that since the level of expression of some matrix molecules varies in osteosarcoma, a better understanding of such molecules might elucidate targets for therapy. In this study, it was demonstrated that HA synthesized by HAS-2 plays important roles in the formation of the pericellular coat, proliferation, motility and invasiveness in MG-63 cells. Another osteosarcoma cell line, HOS, expresses very low HAS mRNA copy number and has very small pericellular coats, but proliferation and invasiveness of these cells are prominent (data not shown). Considering that osteosarcoma as a group has heterogeneous histological features, individual osteosarcoma tissues might have diverse phenotype in HAS expression, and thus the significance of HA in tumorigenesis might also be dependent on the individual osteosarcoma. Not only the proliferation and invasiveness of the tumor, but also the sensitivity to radiotherapy or chemotherapy is quite diverse among osteosarcoma patients. Although not applicable for all osteosarcoma, one implication from this study of the inhibition of HAS-2 in MG-63 suggests the possibility that HAS could be a target molecule for therapy. Analysis of the relationships between expression pattern of HAS and HA and the clinical features in each patient with osteosarcoma would be worthwhile for bridging biological aspects to clinical features of this disease. Better understanding of the significance of HA in each tissue may shed a light on new therapeutic tools, such as made-to-order, patient-specific therapy.

## Acknowledgments

This study was supported in part by the Ministry of Education, Culture, Sports, Science and Technology of Japan (Grant-in-Aid for Scientific Research (C) no. 16591483) and; by NIH grants RO1-AR43384, RO1-AR39507 and P50-AR39239.

## References

1. Link MP, Goorin AM, Miser AW, Green AA, Pratt CB, Belasco JB, Pritchard J, Malpas JS, Baker AR, Kirkpatrick JA, Ayala AG, Shuster JJ, Abelson HT, Simone JV, Veiatti TJ. The effect of adjuvant chemotherapy on relapse-free survival in patients with osteosarcoma of the extremity. *N Engl J Med.* 1986; 314:1600–1606. [PubMed: 3520317]
2. Knudson CB, Knudson W. Hyaluronan-binding proteins in development, tissue homeostasis and disease. *FASEB J.* 1993; 7:1233–1241. [PubMed: 7691670]
3. Knudson, W. Hyaluronan in malignancies. In: Laurent, TC., editor. *The Chemistry, Biology and Medical Applications of Hyaluronan and its Derivatives.* Portland Press; London, UK: 1998. p. 169-179.
4. Delpech B, Maingonnat C, Girand N, Chauzy C, Maunoury R, Olivier A, Tayot J, Creissard P. Hyaluronan and hyaluronectin in the extracellular matrix of human brain tumour stroma. *Euro J Cancer.* 1993; 29A:1012–1017.
5. Setälä LP, Tammi MI, Tammi RH, Eskelinen MJ, Lipponen PK, Agren UM, Parkkinen J, Alhava EM, Kosma VM. Hyaluronan expression in gastric cancer cells is associated with local and nodal spread and reduced survival rate. *Br J Cancer.* 1999; 79:1133–1138. [PubMed: 10098747]
6. Ropponen K, Tammi M, Parkkinen J, Eskelinen M, Tammi R, Lipponen P, Agren U, Alhava E, Kosma VM. Tumor cell-associated hyaluronan as an unfavorable prognostic factor in colorectal cancer. *Cancer Res.* 1998; 58:342–347. [PubMed: 9443415]
7. Auvinen P, Tammi R, Parkkinen J, Tammi M, Agren U, Johansson R, Hirvikoski P, Eskelinen M, Kosma VM. Hyaluronan in peritumoral stroma and malignant cells associates with breast cancer spreading and predicts survival. *Am J Pathol.* 2000; 156:529–36. [PubMed: 10666382]
8. Pirinen RT, Tammi RH, Tammi MI, Paakko PK, Parkkinen JJ, Agren UM, Johansson RT, Viren MM, Tormanen U, Soini YM, Kosma VM. Expression of hyaluronan in normal and dysplastic bronchial epithelium and in squamous cell carcinoma of the lung. *Int J Cancer.* 1998; 79:251–255. [PubMed: 9645346]
9. Anttila MA, Tammi RH, Tammi MI, Syrjanen KJ, Saarikoski SV, Kosma VM. High levels of stromal hyaluronan predict poor disease outcome in epithelial ovarian cancer. *Cancer Res.* 2000; 60:150–155. [PubMed: 10646867]
10. Kimata K, Honma Y, Okayama M, Oguri K, Hozumi M, Suzuki S. Increased synthesis of hyaluronic acid by mouse mammary carcinoma cell variants with high metastatic potential. *Cancer Res.* 1983; 43:1347–1354. [PubMed: 6825105]
11. Yang B, Zhang L, Turley EA. Identification of two hyaluronan-binding domains in the hyaluronan receptor RHAMM. *J Biol Chem.* 1993; 268:8617–8623. [PubMed: 7682552]
12. McBride WH, Bard JBL. Hyaluronidase sensitive halos around adherent cells. *J Exp Med.* 1979; 149:507–515. [PubMed: 762499]
13. Weigel PH, Hascall VC, Tammi M. Hyaluronan synthases. *J Biol Chem.* 1997; 272:13997–14000. [PubMed: 9206724]
14. Spicer AP, McDonald JA. Characterization and molecular evolution of a vertebrate hyaluronan synthase gene family. *J Biol Chem.* 1998; 273:1923–1932. [PubMed: 9442026]
15. Spicer AP, Seldin MF, Olsen AS, Brown N, Wells DE, Doggett NA, Itano N, Kimata K, Inazawa J, McDonald JA. Chromosomal localization of the human and mouse hyaluronan synthase genes. *Genomics.* 1997; 41:493–497. [PubMed: 9169154]
16. Kosaki R, Watanabe K, Yamaguchi Y. Overproduction of hyaluronan by expression of the hyaluronan synthase Has2 enhances anchorage-independent growth and tumorigenicity. *Cancer Res.* 1999; 59:1141–1145. [PubMed: 10070975]
17. Itano N, Sawai T, Miyaishi O, Kimata K. Relationship between hyaluronan production and metastatic potential of mouse mammary carcinoma cells. *Cancer Res.* 1999; 59:2499–2504. [PubMed: 10344764]
18. Itano N, Sawai T, Atsumi F, Miyaishi O, Taniguchi S, Kannagi R, Hamaguchi M, Kimata K. Selective expression and functional characteristics of three mammalian hyaluronan synthases in oncologic malignant transformation. *J Biol Chem.* 2004; 279:18679–18687. [PubMed: 14724275]

19. Liu N, Gao F, Han Z, Xu X, Underhill CB, Zhang L. Hyaluronan synthase 3 overexpression promotes the growth of TSU prostate cancer cells. *Cancer Res.* 2001; 61:5207–5214. [PubMed: 11431361]
20. Nishida Y, Knudson CB, Nietfeld JJ, Margulis A, Knudson W. Antisense inhibition of hyaluronan synthase-2 in human articular chondrocytes inhibits proteoglycan retention and matrix assembly. *J Biol Chem.* 1999; 274:21893–21899. [PubMed: 10419509]
21. Faltz LL, Caputo CB, Kimura JH, Schrode J, Hascall VC. Structure of the complex between hyaluronic acid, the hyaluronic acid-binding region, and the link protein of proteoglycan aggregates from the Swarm rat chondrosarcoma. *J Biol Chem.* 1979; 254:1381–1387. [PubMed: 762134]
22. Knudson CB. Hyaluronan receptor-directed assembly of chondrocyte pericellular matrix. *J Cell Biol.* 1993; 120:825–834. [PubMed: 7678838]
23. Bullard KM, Kim HR, Wheeler MA, Wilson CM, Neudauer CL, Simpson MA, McCarthy JB. Hyaluronan synthase-3 is upregulated in metastatic colon carcinoma cells and manipulation of expression alters matrix retention and cellular growth. *Int J Cancer.* 2003; 107:739–746. [PubMed: 14566823]
24. Evanko SP, Wight TN. Intracellular localization of hyaluronan in proliferating cells. *J Histochem Cytochem.* 1999; 43:1331–1341. [PubMed: 10490462]
25. Nishida Y, D'Souza AL, Thonar EJ, Knudson W. Stimulation of hyaluronan metabolism by interleukin-1 $\alpha$  in human articular cartilage. *Arthritis Rheum.* 2000; 43:1315–1326. [PubMed: 10857790]
26. Hascall VC, Majors AK, De La Motte CA, Evanko SP, Wang A, Drazba JA, Strong SA, Wight TN. Intracellular hyaluronan: a new frontier for inflammation? *Biochim Biophys Acta.* 2004; 1673:3–12. [PubMed: 15238245]
27. Peterson RM, Yu Q, Stamenkovic I, Toole BP. Perturbation of hyaluronan interactions by soluble CD44 inhibits growth of murine mammary carcinoma cells in ascites. *Am J Pathol.* 2000; 156:2159–2167. [PubMed: 10854236]
28. Zoltan-Jones A, Huang L, Ghatak S, Toole BP. Elevated hyaluronan production induces mesenchymal and transformed properties in epithelial cells. *J Biol Chem.* 2003; 278:45801–45810. [PubMed: 12954618]
29. Ghatak S, Misra S, Toole BP. Hyaluronan Oligosaccharides Inhibit Anchorage-independent Growth of Tumor Cells by Suppressing the Phosphoinositide 3-Kinase/Akt Cell Survival Pathway. *J Biol Chem.* 2002; 277:38013–38020. [PubMed: 12145277]
30. Hofmann M, Fieber C, Assmann V, Gottlicher M, Sleeman J, Plug R, Howells N, von Stein O, Ponta H, Herrlich P. Identification of IHABP, a 95 kDa intracellular hyaluronate binding protein. *J Cell Sci.* 1998; 111:1673–1684. [PubMed: 9601097]
31. Collis L, Hall C, Lange L, Ziebell M, Prestwich R, Turley EA. Rapid hyaluronan uptake is associated with enhanced motility: implications for an intracellular mode of action. *FEBS Lett.* 1998; 440:444–449. [PubMed: 9872419]
32. Evanko SP, Angello JC, Wight TN. Formation of hyaluronan- and versican-rich pericellular matrix is required for proliferation and migration of vascular smooth muscle cells. *Arterioscler Thromb Vasc Biol.* 1999; 19:1004–1013. [PubMed: 10195929]
33. Park MJ, Kim MS, Park IC, Kang HS, Yoo H, Park SH, Rhee CH, Hong SI, Lee SH. PTEN suppresses hyaluronic acid-induced matrix metalloproteinase-9 expression in U87MG glioblastoma cells through focal adhesion kinase dephosphorylation. *Cancer Res.* 2002; 62:6318–6322. [PubMed: 12414663]
34. Zhu D, Bourguignon LY. Interaction between CD44 and the repeat domain of ankyrin promotes hyaluronic acid-mediated ovarian tumor cell migration. *J Cell Physiol.* 2000; 183:182–195. [PubMed: 10737894]
35. Bielack SS, Kempf-Bielack B, Dellling G, Exner GU, Flege S, Helmke K, Kotz R, Salzer-Kuntschik M, Werner M, Winkelmann W, Zoubek A, Jurgens H, Winkler K. Prognostic factors in high-grade osteosarcoma of the extremities or trunk: an analysis of 1,702 patients treated on neoadjuvant cooperative osteosarcoma study group protocols. *J Clin Oncol.* 2002; 20:776–790. [PubMed: 11821461]

36. Glasser DB, Lane JM, Huvos AG, Marcove RC, Rosen G. Survival, prognosis, and therapeutic response in osteogenic sarcoma. The Memorial Hospital experience. *Cancer*. 1992; 69:698–708. [PubMed: 1730120]
37. Meyers PA, Heller G, Healey JH, Huvos A, Applewhite A, Sun M, LaQuaglia M. Osteogenic sarcoma with clinically detectable metastasis at initial presentation. *J Clin Oncol*. 1993; 11:449–453. [PubMed: 8445419]
38. Thorpe W, Loeb W, Hyatt C, Rosenberg SA. Alkaline phosphatase measurements of paired normal and osteosarcoma tissue culture lines obtained from the same patient. *Cancer Res*. 1979; 39:277–279. [PubMed: 282939]
39. Gorlick R, Huvos AG, Heller G, Aledo A, Beardsley GP, Healey JH, Meyers PA. Expression of HER2/erbB-2 correlates with survival in osteosarcoma. *J Clin Oncol*. 1999; 17:2781–2788. [PubMed: 10561353]
40. Hernandez-Rodriguez NA, Correa E, Sotelo R, Contreras-Paredes A, Gomez-Ruiz C, Green L, Mohar A. Ki-67: a proliferative marker that may predict pulmonary metastases and mortality of primary osteosarcoma. *Cancer Detect Prev*. 2001; 25:210–215. [PubMed: 11341357]
41. Raymond, AK.; Ayala, AG.; Knuutila, S. Conventional osteosarcoma. In: Kleihues, P.; Sobin, L.; Fletcher, C.; Unni, KK.; Mertens, F., editors. *WHO Classification of Tumours: Pathology and Genetics of Tumours of Soft Tissue and Bone*. IARC Press; Lyon, France: 2002. p. 264-270.

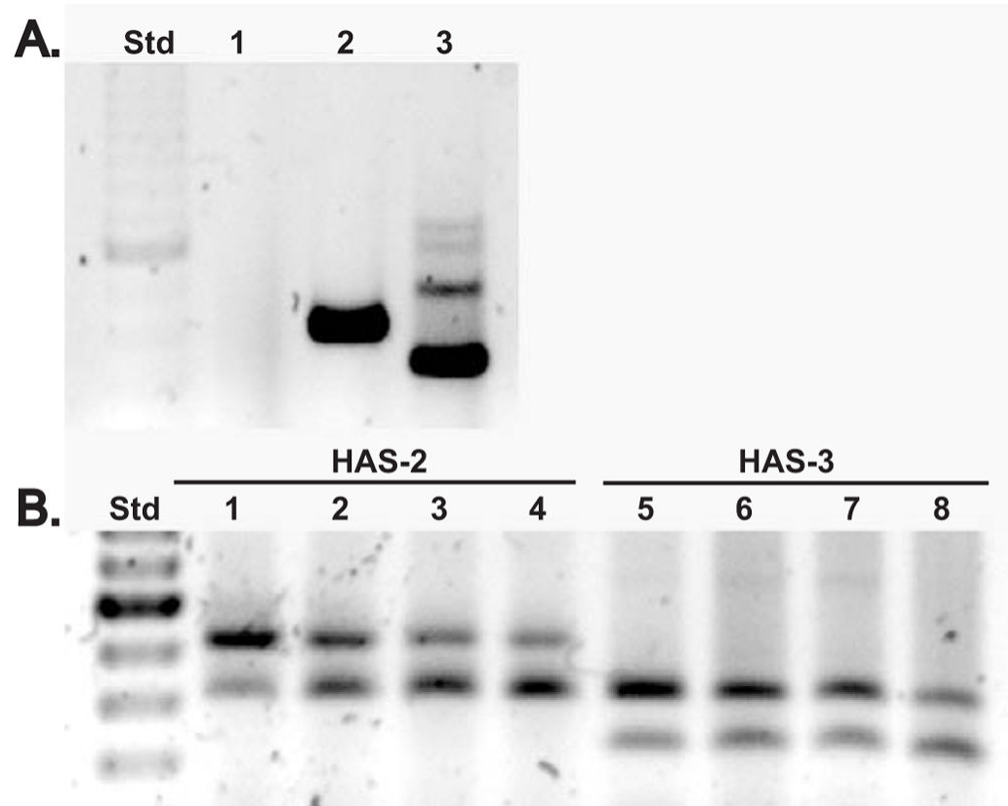


**Figure 1. RT-PCR analysis of HAS mRNA expression in MG-63 cells**

(A) Total RNA isolated from MG-63 cells was reverse-transcribed and PCR amplified for 35 cycles with HAS-1, HAS-2 or HAS-3 specific primers. The products were separated on 1.5% agarose gels and visualized by SYBR Green I staining. Lanes 1–3 represent conventional PCR amplification of HAS-1, HAS-2 or HAS-3, respectively. Lane Std represents 600-bp of 100 base pair DNA ladder marker band. (B) Aliquots (0.125  $\mu$ g) of total RNA were reverse-transcribed and PCR co-amplified with HAS-2 or HAS-3 DNA mimics for 26 cycles with HAS-2 or HAS-3 specific primers, respectively. The slower migrating bands in all lanes are the mimics. Lanes 1–4 represent co-amplification of sample cDNA with 50, 25, 12.5, and 6.25 attomoles of HAS-2 DNA mimic and primers. Lanes 5–8 represent aliquots of the same RNA PCR co-amplified with 2, 1, 0.5, and 0.25 attomol of HAS-3 DNA mimic and HAS-3 primers. The stained products were scanned and quantified using a fluoroimaging system. Std represents 100 base pair DNA ladder markers. HAS-2 target, 409 bp; mimic, 523 bp. HAS-3 target, 331 bp; mimic, 421 bp.

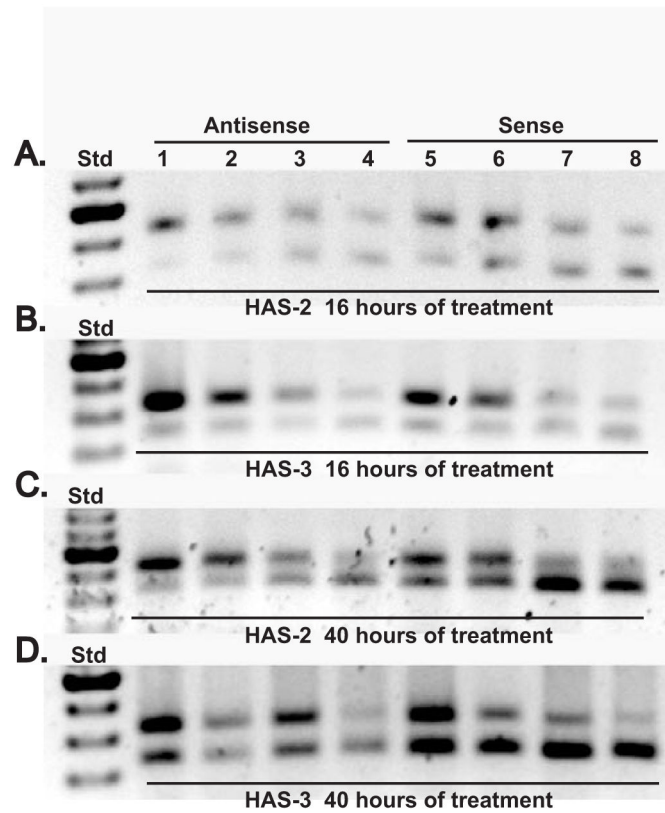


**Figure 2. The effect of HAS-2 antisense oligonucleotide treatment on HAS-2 or HAS-3 mRNA expression by MG-63 cells**

Aliquots of total RNA (0.125  $\mu$ g) derived from MG-63 cells cultures treated with 2  $\mu$ M HAS-2 antisense or control oligonucleotides for varying times (16 and 40 hours after addition of oligonucleotides is shown) were reverse-transcribed and PCR co-amplified for 26 cycles with HAS-2 or HAS-3 mimics and HAS-2 or HAS-3 specific primers, respectively. The products were separated on 1.5% agarose gel and visualized by SYBR Green I staining. The stained products were scanned and quantified using a fluorimaging system. The slower migrating bands in all lanes are the mimics. Panels A and B depict competitive RT-PCR amplification of total RNA isolated from MG-63 cultures treated with HAS-2 antisense oligonucleotides for 16 hours; 40 hour cultures in panels C and D. HAS-2 primers and mimics are shown in panels A and C; HAS-3 primers and mimics in panels B and D. Lanes 1–4 in each panel represent amplification of RNA isolated from HAS-2 antisense oligonucleotide-treated cultures; lanes 5–8, HAS-2 sense oligonucleotides treated cultures. For HAS-2 PCR analyses, lanes 1–4 and 5–8 represent samples co-amplified with 50, 25, 12.5, and 6.25 attomol of HAS-2 DNA mimic, respectively. For HAS-3 PCR analyses, lanes 1–4 and 5–8 represent samples co-amplified with 1, 0.5, 0.25, and 0.125 attomol of HAS-3 DNA mimic, respectively. HAS-2 target, 409 bp; mimic, 523 bp. HAS-3 target, 331 bp; mimic, 421 bp. Std represents 100 base pair DNA ladder markers.

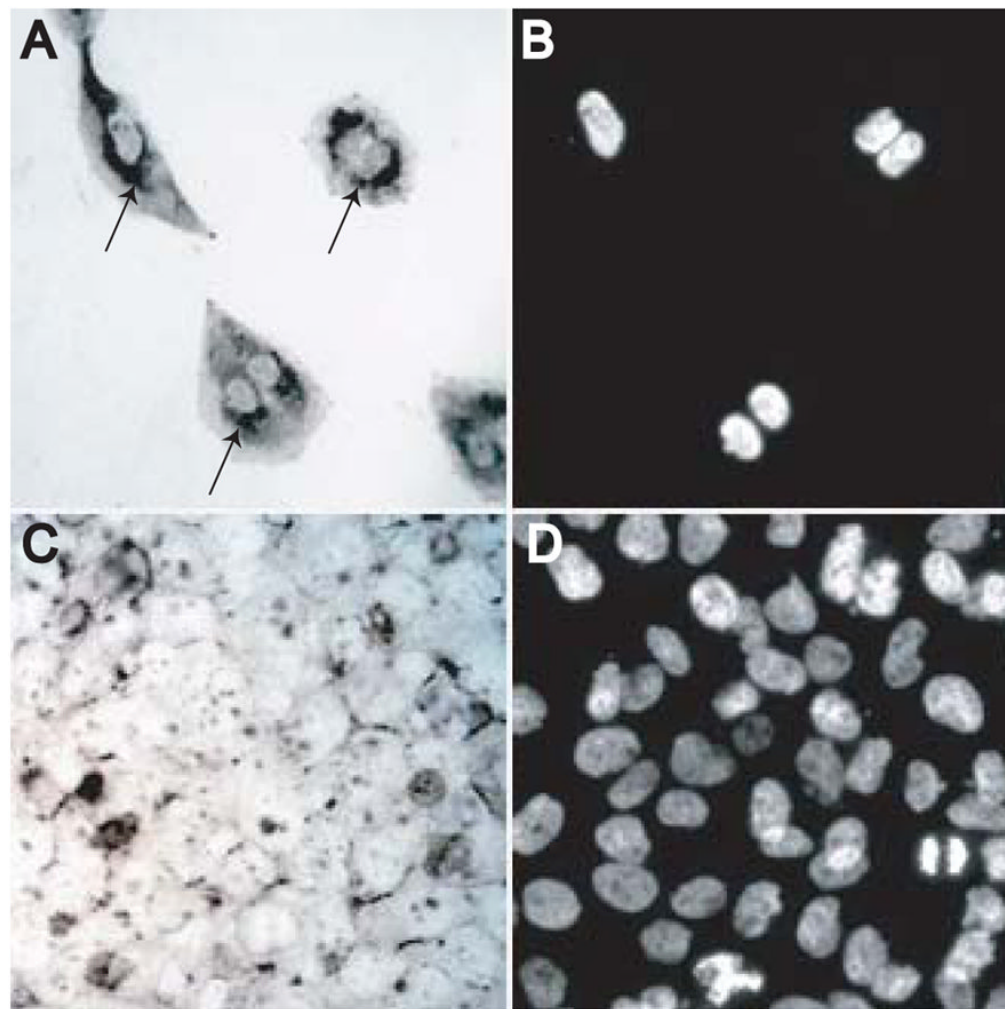


**Figure 3. Hyaluronan accumulation by MG-63 cells during proliferative and confluent growth**  
MG-63 cells cultured in monolayer were fixed in 2% paraformaldehyde and stained for HA using a biotinylated HABP followed by streptavidin peroxidase. Low density cultures in proliferative phase of growth are shown in Panel A; confluent cultures in Panel C. Nuclear staining with DAPI of the same cells shown in panels A and C are shown in panels B and D, respectively. The arrows shown in panel A depict cytoplasmic HABP-positive staining. All cells were photographed and printed at the same magnification. (original magnification: 200x)

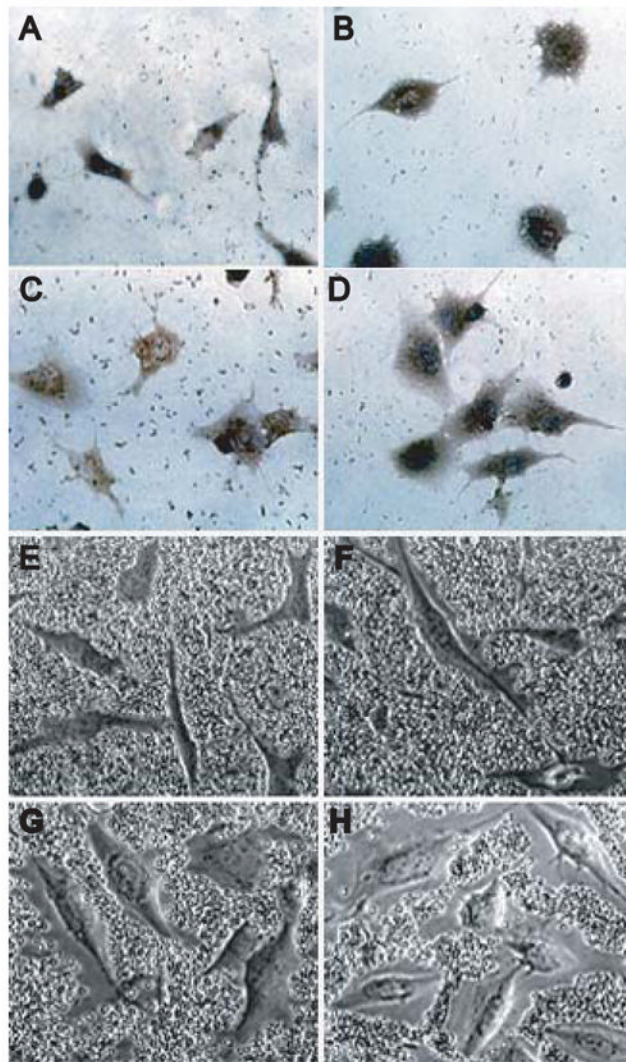


**Figure 4. The effect of HAS-2 antisense oligonucleotides on HA retention in MG-63 cells**  
MG-63 cells were fixed in 2% paraformaldehyde and stained for HA with biotinylated HABP 12 hours (panels A and B) or 24 hour (panels C and D) following the initial addition of HAS-2 antisense (panels A and C) or sense (panels B and D) oligonucleotides. Fixed erythrocytes were applied to cultures of MG-63 cells 16 hours (panels E and F) or 40 hours (panels G and H) following the initial addition of HAS-2 antisense (panels E and G) or sense (panels F and H) oligonucleotides. All cells were photographed and printed at the same magnification. (original magnification: 200x).

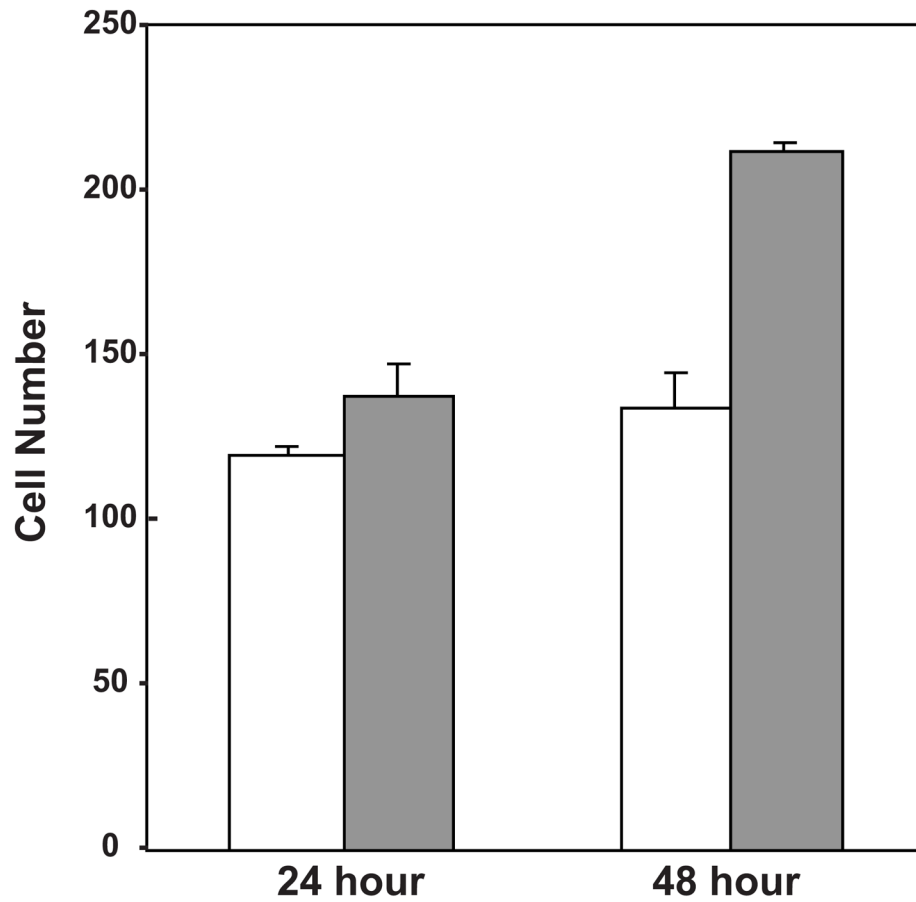


**Figure 5. The effect of HAS-2 oligonucleotides on MG-63 cell proliferation**

MG-63 cells incubated for 24 and 48 hours after initial addition of antisense or sense oligonucleotides were analyzed for changes in cell proliferation by MTT assay. Bars represent the average  $\pm$  s.d. of absorbance values at 570nm. Data was averaged from triplicate experiments. Differences between antisense (open bars) and sense (shaded bars) treatments exhibited statistical significance,  $p=0.012$  and  $p=0.0002$  for data obtained at both 24 and 48 hours post transfection, respectively.

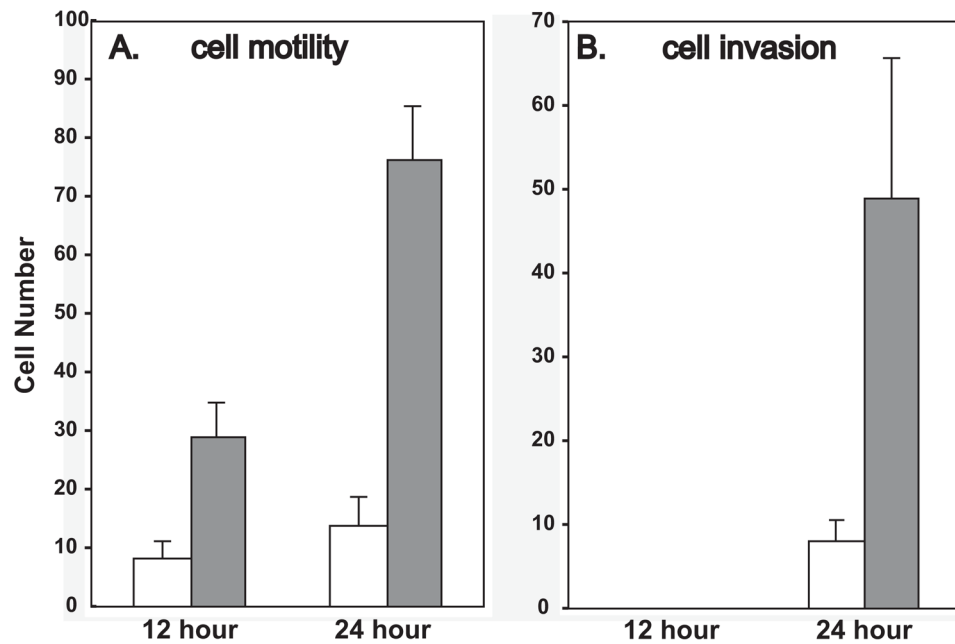


**Figure 6. The effect of HAS-2 antisense oligonucleotides on MG-63 cell motility and invasiveness**  
 Following transfection with antisense or sense oligonucleotides, MG-63 cells were assayed for cell motility and invasiveness through the use of modified Boyden chamber assays without (A) or with matrigel (B) respectively, for an additional 12 and 24 hours. The cells were then fixed with 2% paraformaldehyde and visualized with hematoxylin staining. The number of cells on lower surface of the membrane was calculated in 4 randomly selected high power fields of view. Changes in the number (average  $\pm$  s.d.) of migrating cells after 12 and 24 hours of migration are summarized in panel A. Differences between antisense and sense treatments exhibited statistical significance for data obtained following 12 hours ( $p=0.0066$ ) and 24 hours ( $p=0.00065$ ) of migration. Changes in the number (average  $\pm$  s.d.) of invading cells are summarized in panel B. Differences between antisense (open bars) and sense (shaded bars) treatments exhibited statistical significance with a  $p=0.013$  for data obtained 24 hours post transfection.

**Table 1**

Copy number of HAS-2 and HAS-3 expressed by MG-63 cells treated with antisense or sense oligonucleotides.

	16 hours		40 hours	
	HAS-2	HAS-3	HAS-2	HAS-3
Antisense	4.07 ± 0.85	0.497 ± 0.135	4.63 ± 0.78	0.239 ± 0.068
Sense	8.80 ± 0.125	0.502 ± 0.153	8.04 ± 1.36	0.267 ± 0.059

Values are the average ± s.d. copy number of mRNA expressed by MG-63 cells normalized by  $10^3$  mRNA copies of expressed GAPDH from 3 separate experiments.